The Journal of the Korean Society of
Coastal and Ocean Engineers
Vol. 4, No. 3, pp. 178~186, September 1992

# Breaking Wave Generation in the Laboratory
# 實驗室에서의 碎波發生

Won Chul Cho* and Michael Bruno*
조원철* · 마이클 부르노*

**Abstract** □ An experimental study of deep-water breaking waves are performed by superposition of different wave frequencies, faster waves overtaking slow waves at a certain location. Large spilling and plunging breaking waves are generated near the expected breaking location. Wave steepness in spilling and plunging breakers significantly increases as the breaking point is approached and then decreases after breaking. Larger growth rate of the wave steepness in vigorous plunging breaking is observed. The fundamental wave frequencies in a wave group are dominant through the wave evolution, even in an intense plunging breaking event.

**要 旨** : 어떤 特定 位置에서 波速이 빠른 波가 느린 波를 추월하도록 여러가지 다른 周波數의 波를 重疊시킴으로써 深海碎波에 대한 實驗을 수행하였다. 예상 碎波지점 근처에서 큰 波高를 갖는 崩壞波와 卷波를 造波시켰다. 碎波點에 가까워 질수록 崩壞波와 卷波의 波形傾斜가 뚜렷하게 增加되었고 碎波 후에는 減少되었다. 격렬한 卷波시에는 波形傾斜가 보다 더 증가됨을 볼 수 있었다. 波群 중의 基本的인 周波數들은 波浪의 傳播過程이나, 특히 격렬한 卷波시에도 별 변동이 없었다.

## 1. INTRODUCTION

Breaking waves in deep water are important in many areas of ocean science and technology. Wave breaking is important in the transfer of energy from the wave field to wind-generated surface currents. It also generates intensive turbulence within the underlying flow field, which mixes the upper layer of the ocean and enhances the transfer of heat and momentum across the air-sea interface. In an oil spill, turbulence generated by breaking waves breaks up oil slicks into many sizes of droplets and drives them to sub-surface depths. Wave breaking is also important in the design of marine structures and in ship hydrodynamics, since the force produced by breaking waves may cause considerable damage to marine structures and vessels.

In the breaking region, the wave profile is transformed in both its length and amplitude as it propagates, until the crest either spills or plunges forward. This evolution can be driven by varying water depth, interaction with a mean current, or interaction with other components in a wave packet.

Most experimental studies on breaking waves have been concerned with waves in shallow water, where the type of breaking is essentially dependent on the bottom slope. Some studies on breaking waves in deep water have been reported and there have been significant advances in recent years. However, knowledge of the asymmetric and highly nonlinear phenomena of breaking waves is not complete.

In 1974, Longuet-Higgins developed a method, 'Storm Building', to generate breaking waves in the laboratory, which requires the generation of waves with decreasing wave frequency, so that the faster waves overtake slow waves at some distance away from the wave paddle, summing up to produce a steep and unstable wave. Kjeldsen and Myrhaug (1979) analyzed extremely unstable waves just

*스티븐스工 大土木 및 海洋工學科(Department of Civil and Ocean Engineering, Stevens Institute of Technology, Hoboken, New Jersey, 07030)

before breaking using the zero-downcross method. They found that the crest front steepness (the crest elevation above mean water level/the horizontal distance from the zero-upcross to the wave crest) was the most important factor in deciding the type of breaking wave, and breaking occurred in the range of front wave steepness between 0.32 and 0.78 (the highest value for a plunging breaker). Duncan *et al.* (1987) also analyzed breaking waves using the crest front steepness, and found that the crest front steepness increased slowly up to the breaking point and then decreased during the beginning of the breaking process with the average value of 0.5 for a spilling breaker and 0.7 for a plunging breaker.

In the present study, we will also use Longuet-Higgin's method to investigate the evolution of spilling and plunging breaking waves, generating a wave group by decreasing the wave frequency with increasing wave amplitude.

## 2. THEORY

It was shown by Longuet-Higgins (1974) that wave trains with decreasing frequencies converge at a single point in time and space. He developed this concept using linear wave theory in deep water.

The phase velocity of a gravity wave train is

$$C=\frac{gT}{2\pi}\tanh\left(\frac{2\pi h}{L}\right) \tag{1}$$

where g: gravitational acceleration
T: wave period
L: wave length
h: water depth

Since $\tanh 2\pi h/L \rightarrow 1$ in deep water, the phase velocity in deep water is

$$\frac{gT}{2\pi}=\frac{g}{2\pi f} \tag{2}$$

where f: wave frequency (Hz)

The wave energy propagates with the group velocity, which is equal to 1/2 of the phase velocity in deep water

$$C_g=\frac{C}{2}=\frac{g}{4\pi f} \tag{3}$$

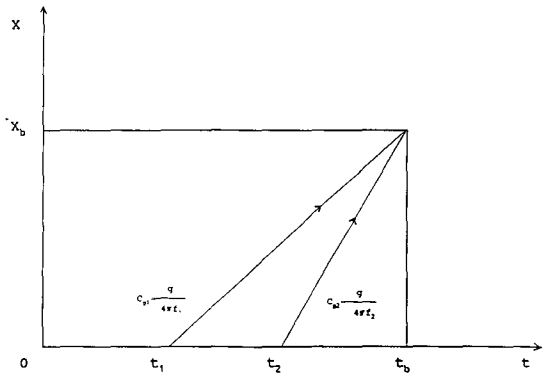


**Fig. 1.** Convergence of two wave groups of different frequencies.

Therefore, the longer wave with lower frequency propagates faster so that it overtakes a shorter wave at a time $t_b$ and at a distance $X_b$ if the higher frequency wave is started first. The wave energy also converges at this point, and breaking may occur. Referring to Fig. 1, the time to convergence, $t_b$, can be determined as follows:

$$C_{g1}=\frac{X_b}{t_b-t_1}=\frac{g}{4\pi f_1}$$
for the high frequency wave (4)

$$C_{g2}=\frac{X_b}{t_b-t_2}=\frac{g}{4\pi f_2}$$
for the low frequency wave (5)

By eliminating $t_b$ from the above two equations:

$$t_2-t_1=\frac{4\pi X_b}{g}(f_1-f_2) \tag{6}$$

$$\frac{f_2-f_1}{t_2-t_1}=-\frac{g}{4\pi X_b} \tag{7}$$

If the wave frequency, f, is varied continuously so that

$$\frac{df}{dt}=\mathrm{Lim}_{\Delta t\rightarrow 0}\frac{f_2-f_1}{t_2-t_1}=-\frac{g}{4\pi X_b} \tag{8}$$

then the energy of two waves of different frequency converge at a distance $X_b$ from the wavemaker and $X_b$ is dependent on the frequency difference between the two waves.

## 3. EXPERIMENT

### 3.1 Experimental apparatus

The breaking wave experiments were performed at Davidson Laboratory of Stevens Institute of Technology, where the wave channel is 313 feet long, 12 feet wide, and the water depth is 5.4 feet.

The wave channel is equipped with a dual-flap hydraulic wavemaker at one end and a wave absorbing beach at the other. The dual flap is composed of a lower flap and an upper flap in which the lower flap is hinged on the channel floor and the upper flap is hinged on the top of the lower flap. The wavemaker is controlled by PDP-11 microcomputer which calculates the digital signal form of flap amplitude as a function of time for a given wave frequency and height. These digital time series are converted to control voltage corresponding to the stored digital sequence at a predetermined time interval through the digital-to-analog converter. Then, the hydraulic servo system produces a specific wave form proportional to the applied sinusoidal flap angles. Since the wavemaker control is accomplished by programming the microcomputer, appropriate computer programming allows one to generate a regular wave, random wave, and virtually any other type of wave form.

The wooden sloping beach at the end opposite the wavemaker dissipates propagating waves and absorbs incident wave energy to minimize wave reflection during tests. Owing to the relatively long wave channel and the short duration of each test, the waves were not disturbed by reflection from the beach, which may yield slow modulations to the incident waves. Measurements were in all cases completed within 1 minute before wave energy was reflected to the measuring station. Data collection was begun just after turning on the wavemaker. All tests were started after calm water was obtained, with the usual time to calm water between two runs taken appoximately 30 minutes.

Six wave gauges were used for the measurement of the waves in the spilling and plunging breaking waves tests. These gauges were installed at different measuring stations, since the predicted breaking locations were varied according to the wave frequency decrement rate-measuring stations at 20, 35, 50, 65, 80, and 95 ft for breaking waves at 73 ft from the wavemaker; at 20, 45, 70, 95, 120, and 145 ft for breaking waves at 102 ft; and at 20, 50, 80, 110, 140, and 170 ft for breaking waves at 128 ft. Wave gauges were calibrated daily using vertical traverse mechanisms mounted above the water surface in the wave channel. There was only negligible differences in each calibration. The data acquisition/processing system is designed for various types of tank tests at Davidson Laboratory. The data acquisition program digitizes analog signals from the instruments by an analog-to-digital converter at a selected rate, and records them on the disk in digital form as the test progresses. The spectral analysis program, which contains Fast-Fourier-Transform processing, calculates the energy density spectrum of the signal recorded in a time history file.

### 3.2 Experimental parameters of breaking waves

The technique used in this experiment is described by Longuet-Higgins (1974) and involves by decreasing the frequency and increasing the amplitude of successive waves. Three different wave frequency decrement rates, df=0.02 Hz, 0.025 Hz and 0.035 Hz, which are the main factors in deciding the breaking location, were used for breaking waves occurring at different breaking locations at 128 ft, 102 ft and 73 ft, respectively (refer to Section 2). Three different wave frequency ranges with each wave frequency decrement rate were also examined to observe the effect of the initial wave steepness in the breaking process. Wave amplitude was increased linearly by a specified wave amplitude increment factor (0.15 was used for this experiment). A wave group of decreasing wave frequency and increasing amplitude is therefore generated, which can be represented in the following way:

$$\begin{aligned}\eta_n &= a_n \sin(2\pi f_n t)\\ &= a_n \sin[2\pi(f-(n-1)df)t] \qquad (9)\\ n &= 1,\ 2,\ 3,\ldots.8\end{aligned}$$

where $a_n$: wave amplitude in inches for each wave $=(H/2)(0.1+0.15(n-1))$

H: wave height factor in inches

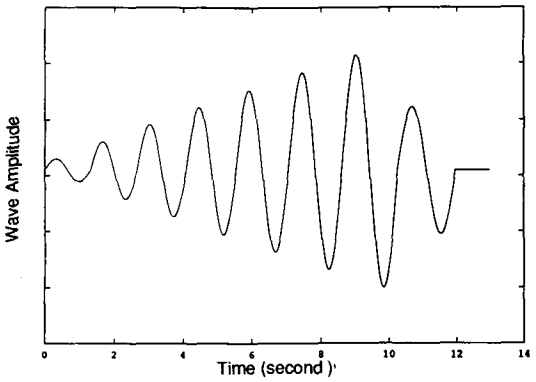


**Fig. 2.** A wave group of decreasing wave frequency and increasing amplitude.

An example of the time history of wave amplitude for such a wave group is shown in Fig. 2.

## 4. RESULTS

### 4.1 Laboratory observations

A wave group, short waves followed by long waves with linearly increasing wave amplitude and constant wave frequency decrement rate, was generated for large spilling and pluging breaking waves tests. The average wave steepness, $ka_{ave}=2\pi(a_{ave}/L_{ave})$, was used for describing the wave steepness in each wave group in a convenient way. As the wave envelope propagated down the wave channel, the wave train was greatly modulated in its shape, with decreasing wave length and period, and reached a maximum steepness near the predicted breaking location, $X_b$, and then dispersed downstream after breaking. The type of breaking wave, spilling or plunging, was decided not only by the initial wave amplitude and wave frequency range (which are the main factors for initial wave steepness) but also by the wave frequency decrement rate, which also controls the breaking location.

Breaking did not occur at small wave amplitudes, although there appeared to be a rapid growth of the wave steepness near the predicted breaking location. As the wave amplitude was increased with a fixed wave frequency range and frequency decrement rate, leading to larger initial wave steepness, a weak spilling breaker occurred approximately one wavelength after the predicted breaking location (re-

**Table 1.** Laboratory observation of spilling and plunging breaking waves

| Wave frequency(Hz) | | Wave freq. | Wave Height | Breaking | Breaking | Breaking |
|---|---|---|---|---|---|---|
| Start freq. | End freq. | decrement | factor(inch) | location(ft) | type | intensity |
| 0.75 | 0.61 | 0.02 | 12.4 | 130 | Spilling | Weak |
| | | | 13 | 126 | Plunging | Weak |
| 0.73 | 0.59 | 0.02 | 15.2 | 128 | Spilling | Weak$^+$ |
| | | | 15.5 | 125 | Plunging | Weak$^+$ |
| 0.71 | 0.57 | 0.02 | 16 | No breaking | | |
| 0.785 | 0.61 | 0.025 | 11.4 | 110 | Spilling | Moderate |
| | | | 11.7 | 102 | Plunging | Moderate$^-$ |
| 0.76 | 0.585 | 0.025 | 14.3 | 103 | Spilling | Moderate |
| | | | 15 | 95 | Plunging | Moderate |
| 0.735 | 0.56 | 0.025 | 14.3 | 103 | Spilling | Moderate |
| | | | 15 | 95 | Plunging | Moderate |
| 0.735 | 0.56 | 0.025 | 15.5 | No breaking | | |
| 0.855 | 0.61 | 0.035 | 9.9 | 76 | Spilling | Moderate |
| | | | 10.2 | 70 | Plunging | Moderate |
| 0.82 | 0.575 | 0.035 | 13.2 | 74 | Spilling | Moderate$^+$ |
| | | | 14 | 65 | Plunging | Strong |
| 0.785 | 0.54 | 0.035 | 15 | No breaking | | |

fer to Table 1). At larger wave amplitudes, an intensified spilling breaker occurred near the predicted breaking location. At still larger wave amplitudes, a plunging breaker was produced near or one wavelength before the predicted breaking location, with strong breaking intensity and a sudden drop of wave amplitude after breaking. It was also observed that as the wave amplitude increment rate was increased at the same wave height factor, waves quickly became unstable and breaking occurred far before the predicted breaking point.

As the wave frequency range was increased by one wave frequency decrement rate, i.e., wave frequency range from f=0.76-0.585 Hz to f=0.785-0.61 Hz, with the same wave frequency decrement rate, df=0.025 Hz (the predicted breaking location, $X_b$= 102 ft from the wavemaker), shorter and steeper waves were produced that broke far before the predicted breaking location due to the large initial wave steepness. In these cases, two or three breaking events spaced roughly one wavelength apart were observed. This deviation in the breaking location was adjusted by modifying the initial wave amplitude (and therefore, the initial wave steepness), and spilling and plunging breakers were produced at relatively small wave amplitude at the higher wave frequency range. When the wave frequency range was lowered by one wave frequency decrement rate, i.e., f=0.735-0.56 Hz, waves became nearly unstable near the predicted breaking location, but breaking hardly occurred even at relatively large amplitudes.

At the large wave frequency decrement rate, df= 0.035 Hz ($X_b$=73 ft), breaking occurred earlier at the large wave amplitude, but at the smaller wave amplitudes, either a spilling breaker occurred near or after the predicted breaking location or a plunging breaker was triggered near or before the breaking location as before. At the small wave frequency decrement rate, df=0.02 Hz ($X_b$=128 ft), behavior similar to that observed in the tests with df=0.025 Hz were found, but weak breaking occurred at these relatively large wave amplitudes due to wave energy dissipating through long distance from the wavemaker.

### 4.2 Time history of spilling and plunging breaking waves

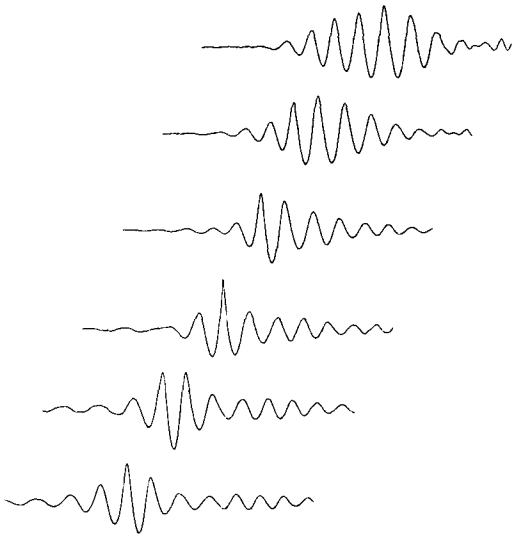

**Fig. 3.** Time history of spilling breaking wave. Wave group parameters f=0.76-0.585 Hz, $ka_{ave}$=0.17, df= 0.025 Hz, and $X_b$=102 ft from the wavemaker. Measuring stations at 20, 45, 70, 95, 120, and 145 ft from the wavemaker. Actual breaking location around 103 ft.

In a comparison of the time history of the wave evolution of spilling and plunging breaking waves, the two wave groups exhibit similar wave profiles initially, with slowly progressing wave-wave interaction. However, as the wave envelope approaches the breaking location, the spilling breaking wave (Fig. 3) has a nearly symmetric wave profile about the peak wave, while the plunging breaking wave (Fig. 4), has a somewhat asymmetric profile with a steeper front face. These breaking profiles were also observed by Rapp (1987) in his laboratory experiments on spilling and plunging breaking waves. The discrepancy is also displayed just after breaking since each breaker has a different breaking location, intensity and distance with stronger breaking intensity and longer breaking distance in a plunging breaker. Two peak wave amplitudes are observed for a spilling breaker, the first one corresponding to the broken spilling wave and the second one corresponding to the wave following the broken wave. A large peak wave is observed for a plunging breaker since, because of the earlier breaking event, the wave following the broken wave overtakes the broken wave soon after the breaking event. Slightly

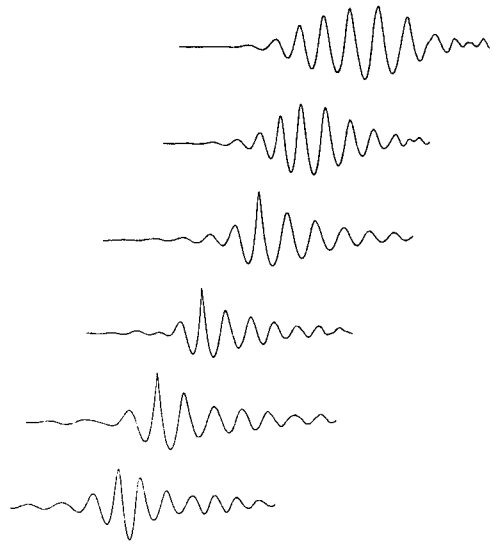

**Fig. 4.** Time history of plunging breaking wave. Wave group parameters f=0.76-0.585 Hz, $ka_{ave}$=0.178, df=0.025 Hz, and $X_b$=102 ft from the wavemaker. Measuring stations at 20, 45, 70, 95, 120, and 145 ft from the wavemaker. Actual breaking location around 95 ft.

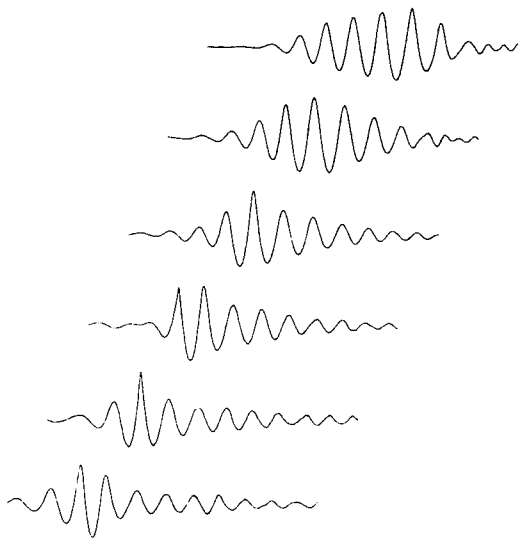

**Fig. 5.** Time history of nonbreaking wave. Wave group parameters f=0.76-0.585 Hz, $ka_{ave}$=0.166, df=0.025, and $X_b$=102 ft from the wavemaker. Measuring stations at 20, 45, 70, 95, 120, and 145 ft from the wavemaker.

different wave profiles are exhibited after the breaking region. In the nonbreaking waves, similar wave

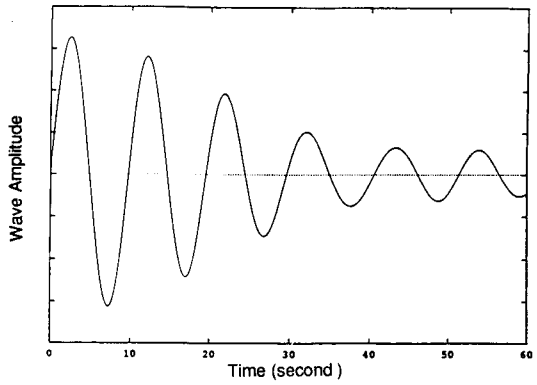


**Fig. 6.** Time history of the calculated wave envelope. Wave group parameters f=0.76-0.585 Hz, $ka_{ave}$=0.178, and df=0.025 Hz.

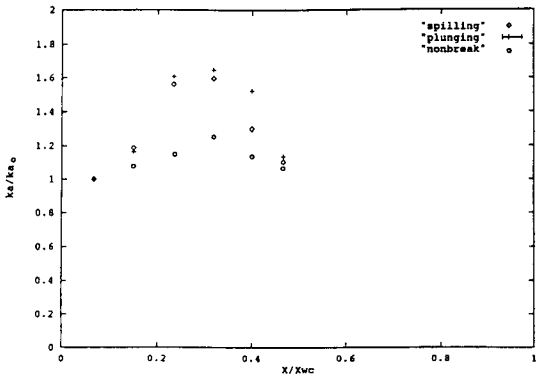


**Fig. 7.** Variation of the wave steepness along the wave channel. Wave group parameters f=0.76-0.585 Hz, df=0.025 Hz, $X_b$=102 ft, and $ka_{ave}$=0.166 (nonbreaking, ○), 0.17 (spilling, ) and 0.178 (plunging, +). Measuring stations at 20, 45, 70, 95, 120, and 145 ft from the wavemaker.

profiles (Fig. 5) are exhibited with a nearly unstable front face as the wave approaches the breaking location, but not enough to lead to breaking.

There appears to be good agreement in the comparision between the measured wave profile at the initial stage (the wave profile at x=45 ft in Fig. 3 and 4) and the computer-generated wave profile shown in Fig. 6.

### 4.3 Variation of the wave steepness along the wave channel

The variation of the non-dimensionlized wave steepness, $ka/ka_0$, where $ka_0$ is the steepness nearest

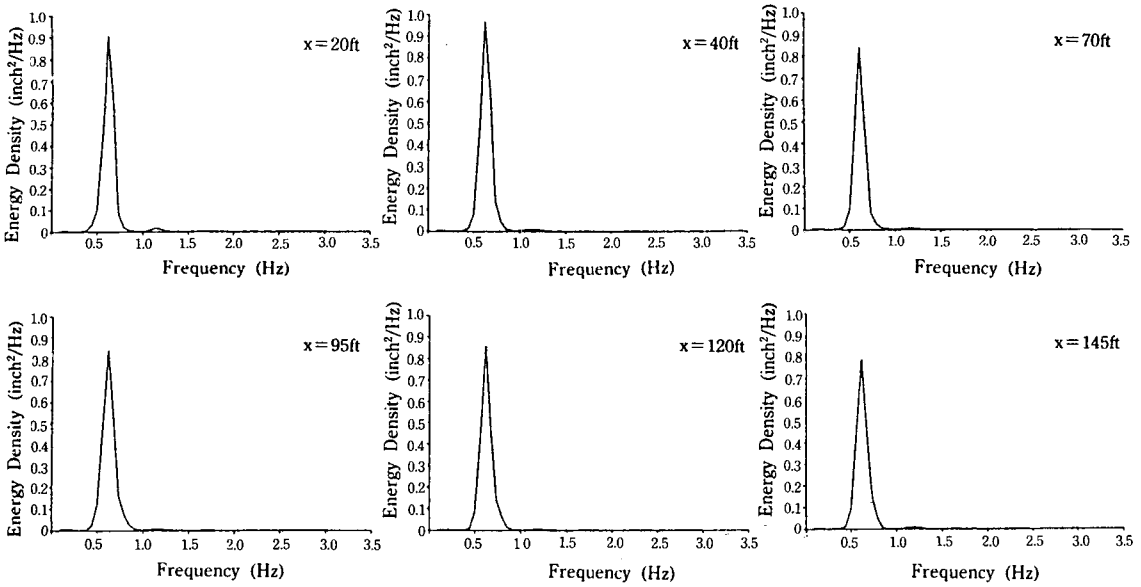


**Fig. 8.** Evolution of energy density spectrum of nonbreaking wave. Wave group parameters f=0.76−0.585 Hz, $ka_{ave}$=0.166, df=0.025 Hz, and $X_b$=102 ft from the wavemaker.

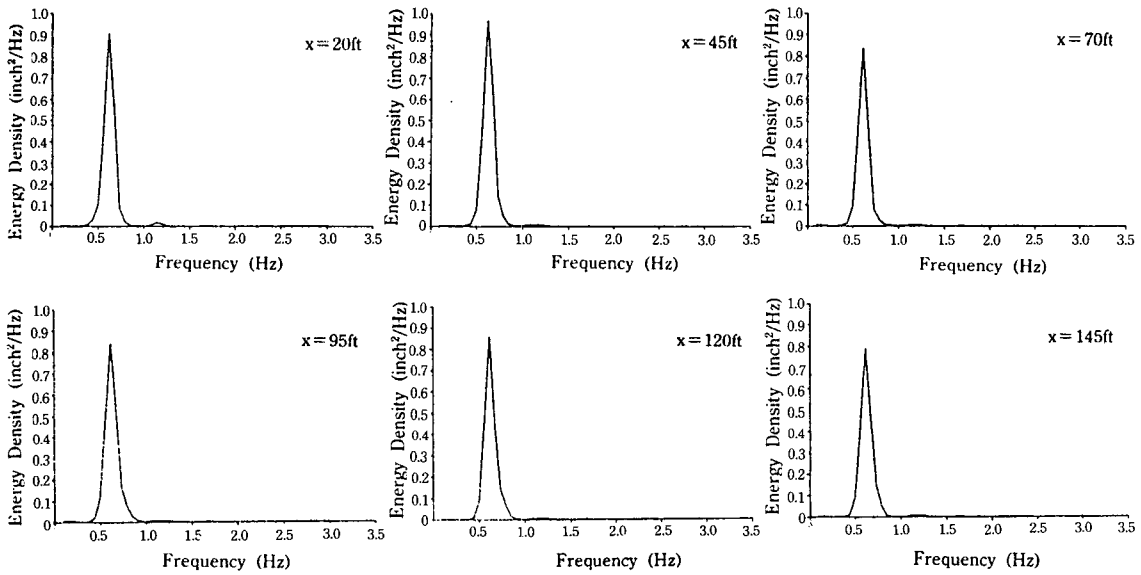


**Fig. 9.** Evolution of energy density spectrum of plunging breaking wave. Wave group parameters f=0.76−0.585 hz, $ka_{ave}$= 0.178, df=0.025 Hz, and $X_b$=102 ft from the wavemaker.

the wavemaker, for the peak wave in a wave group is shown in Fig. 7. The wavenumber, k, and wave amplitude, a, are determined using the dominant wave frequency and peak wave amplitude in each wave envelope. The x-axis is the distance of the measurement station from the wavemaker normalized by the length of the wave channel, $X_{wc}$. Relatively small wave steepness variation is shown in a nonbreaking wave, with a slight, nearly linear increase in wave steepness as the predicted breaking location is approached, followed by a linear decrease. A strong variation of wave steepness before

breaking is observed in both spilling and plunging breaking waves. The wave steepness reaches its maximum just before breaking. After breaking, the wave steepness decreases rapidly, but remains larger than the initial wave steepness. In the case of the plunging breaking wave, the wave steepness increases more rapidly than that of the spilling breaking wave before breaking. A much faster decrease in wave steepness after breaking is exhibited in the spilling breaking process.

### 4.4 Evolution of the energy density spectrum

The energy density spectra are shown in Fig. 8 and 9 (for nonbreaking wave and plunging breaking wave, respectively). In both cases, the fundamental wave frequencies are dominant over the entire wave evolution. In the case of the plunging breaking wave, the waves propagate to the breaking location without losing energy. However, decreased wave energy (approximately 10%) is exhibited after the breaking event. The energy density spectrum of the nonbreaking wave also shows a small ,a loss of wave energy as waves propagate through the predicted breaking location, although further loss of wave energy is not observed.

## 5. CONCLUSION

We have performed deep-water breaking wave tests by wave superposition as faster waves with higher wave frequencies overtake short waves with low wave frequencies at a certain location in time.

Large spilling and plunging breaking waves were generated at or near a certain predicted breaking location in the wave channel. Spilling breaking waves were produced near or one wavelength after the predicted breaking location with a relatiely symmetric wave profile before breaking, while plunging breaking waves were produced near or one wavelength before the predicted breaking location with an asymmetric wave profile about the peak wave. Breaking does not occur at small initial wave steepness. Intense plunging breaking waves are generated a short distance from the wavemaker as the frequency decrement rate or wave amplitude increment rate is increased. At the large frequency decrement rate, a plunging breaker is generated with a relatively small wave amplitude, while a weak spilling breaker is generated with large wave amplitude at the small frequency decrement rate. Wave steepness is increased rapidly as waves approach the predicted breaking location, and then falls off after breaking. In the analysis of energy spectrum, breaking and nonbreaking waves show nearly similar spectrum evolution, but the loss of energy in a plunging breaking wave is greater than that of a nonbreaking wave. The fundamental wave frequencies are always dominant through the wave evolution, even in the intense plunging breaking region.

## REFERENCES


Battjes, J.A. and Sakai, T., 1981. Velocity field in a steady breaker, *J. Fluid Mech.* **65**: 647-656.

Bouwmeester, R.J.B. and Wallace, R.B., 1986. Dispersion of oil on a water surface due to wind and wave action, Report No. DOT/OST/P-34/87/060. U.S. Dept. of Transportation.

Dean, R.G. and Dalrymple, R.A., Water wave mechanics for engineers and scientists: Wavemaker theory, Prentice-Hall, 170-186.

Dommermuth, D.G., Yue, D.K.P., Lin, W.M., Rapp, R.J., Chan, E.S. and Melville, W.K., 1988. Deep-water plunging breakers: a comparision between potential theory and experiments, *J. Fluid Mech.* **189**: 423-442.

Duncan, J.H., Wallendorf, L.A. and Johnson, B., 1987. An experimental investigation of the kinematic of breaking waves, Report No. EW-7-87, U.S. Naval Academy.

Kjeldsen, S.P. and Myrhaug, D., 1979. Breaking waves in deep water and resulting wave forces, *Proc. 11th offshore Technology Conf.* Houston, Texas, paper No. 3646.

Longuet-Higgins, M.S., 1974. Breaking waves in deep or shallow water, *Proc 10th Conf. on Naval Hydrodynamics*, 597-605.

Milgram, J.H., Donnelly, R.G., Van Houston, R.J. and Camperman, J.M., 1978. Effects of oil slick properties on the dispersion of floating oil into the sea, Report No. CG-D-64-78, U.S. Coast Guard, Washington D.C.

Mizuguchi, M., 1986. Experimental study on kinematics and dynamics of wave breaking, *Proc. 20th Conf. on Coastal Engineering*, 589-603.

Okayasu, A., Shibayama, T. and Mimura, N., 1986. Velocity field under plunging waves, *Proc. 20th Conf. on Coastal Engineering*, 660-674.

Peregrine, D.H., 1983. Breaking waves on beaches, Ann. Rev. Fluid Mech. **15**: 149-178.

Raj, P.P.K., 1977. Theoretical study to determine the sea state limit for the survival of oil slicks on the ocean, Report No. CG-D-90-77, U.S. Coast Guard.

Rapp, R.J. 1986. Laboratory measurements of deep water breaking waves, Ph.D Thesis at M.I.T.

Sakai, T. and Iwagaki, Y., 1978. Estimation of water particle velocity of breaking waves, *Proc. 16th Conf. on Coastal Engineering*, 551-568.

Salsich, J.O., Johnson, B. and Holton, C., 1983. A transient wave generation technique and some engineering applications, *Proc. 20th ATTC*, Hoboken, NJ, 949-968.